

AperTO - Archivio Istituzionale Open Access dell'Università di Torino

Unveiling the interaction between PDT active squaraines with ctDNA: A spectroscopic study

This is a pre print version of the following article:

Original Citation:

Availability:

This version is available <http://hdl.handle.net/2318/1790927> since 2021-06-17T12:08:14Z

Published version:

DOI:10.1016/j.saa.2020.119224

Terms of use:

Open Access

Anyone can freely access the full text of works made available as "Open Access". Works made available under a Creative Commons license can be used according to the terms and conditions of said license. Use of all other works requires consent of the right holder (author or publisher) if not exempted from copyright protection by the applicable law.

(Article begins on next page)

Unveiling the interaction between PDT active squaraines with ctDNA: a spectroscopic study

Cosmin Butnarusu^a, Nadia Barbero^b Guido Viscardi^b and Sonja Visentin^a

^a University of Torino, Department of Molecular Biotechnology and Health Science, Via Quarellotto 15, 10135 Torino, Italy

^b University of Torino, Department of Chemistry and NIS Interdepartmental Centre, Via Pietro Giuria 7, 10125 Torino, Italy

*Corresponding author: Sonja Visentin, sonja.visentin@unito.it

Keywords: DNA, squaraines, photodynamic therapy (PDT), interaction, groove binders

ABSTRACT

Squaraine dyes are potential photosensitizers in photodynamic therapy (PDT) due to their ability to release reactive oxygen species (ROS) and cause DNA damage. For this reason, the evaluation and determination of the type of interaction between squaraines and DNA is of the utmost importance.

In this study different spectroscopic techniques such as UV-Vis and fluorescence spectroscopies were used to investigate the type of interaction that occurs between two photosensitizers (halogenated squaraines, i.e. Br-C4 and I-C4) and calf thymus DNA (ctDNA). Squaraines were found to bind ctDNA externally following a minor groove binding as they were able to replace Hoechst (a classic groove binder) from the groove of DNA. This binding mode was further supported by iodide quenching studies, ionic strength assay and [Fluorescence Resonance Energy Transfer](#). Moreover, association (K_A) and dissociation (K_D) constants were obtained and compared with constants of well-known groove binders.

1. Introduction

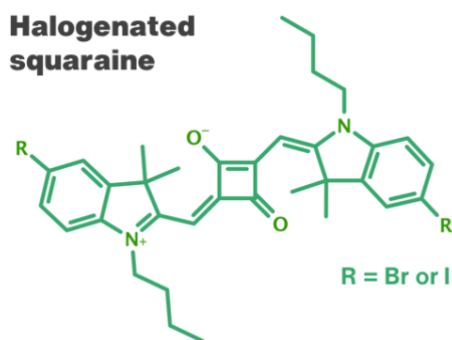
The living organisms encloses all the genetic information useful for their development and functioning within deoxyribonucleic acid (DNA). As DNA is the key component for organisms well-being, from a pharmaceutical point of view DNA is a central target for most oncologic drugs, as

40 well as many antiretroviral and antimicrobial agents [1]. Based on the mechanism of interaction
41 with DNA, drugs are distinguished between groove-binders, intercalating, strand-breaking and
42 covalent bonding [2]. Some of these drugs generates harmful reactive oxygen species (ROS)
43 capable to produce DNA damage. Proteins, lipids and nucleic acids are the biological targets of
44 ROS. The alteration induced by ROS usually produce disfunctions of normal activities of the
45 biological targets and that brings eventually to cell death [3,4]. From a clinical point of view the
46 generation of ROS in specific and defined target points in the human body are of utmost
47 importance in photodynamic therapy (PDT). PDT encompasses the topical or systemically
48 administration of a photosensitizer which, after irradiation at an appropriate wavelength, is
49 capable of producing ROS, resulting in damage to target cancer cells in which it is selectively
50 accumulated [3,5]. Recently our group synthesized and studied some series of polymethine dyes
51 demonstrating their ability to release ROS [6,7]. It was shown that in particular two squaraines
52 named Br-C4 and I-C4 are potential photosensitizers for PDT (Figure 1) [6].

53 Squaraine dyes are the products of dicondensation reactions between electron-rich substrates
54 and squaric acid. In the last two decades great interest was addressed to this class of organic
55 dyes because of their interesting photochemical and photophysical characteristics. Indeed,
56 squaraines display an intense absorption and emission in the red to near infrared region. These
57 photophysical features raised their use in a huge amount of technologies, such as renewable
58 energy [8–11], biological applications [6,12–15] and sensitizers for PDT [5,16,17]. Moreover,
59 different studies have proved that while in dark conditions squaraines are hardly cytotoxic, after
60 irradiation at proper wavelength, they induced a significative phototoxic activity in cancer cells,
61 which was proportional to the squaraine concentration [5,16].

62 Since small compounds can interact with the double strand of DNA in different ways, it is essential
63 to decipher the mechanism of interaction at molecular level in order to design novel and promising
64 drugs for clinical use. Intercalators and groove binders behave differently with the genetic
65 material: the intercalators insert into the double helix, forming a stronger and more damaging
66 bond with DNA than groove binders. The groove binders, on the other hand, remain on the outside
67 of the double helix, bonding in a less powerful manner; anyway, this still causes DNA damage
68 even if to a lesser extent. These differences on the binding with DNA allow us to discriminate the
69 various bonds through the use of spectrophotometric techniques. Although several papers have
70 been published concerning the photodynamic activity of halogenated squaraines and their
71 damage to DNA [6,16,18], little is known about their mechanism of interaction with DNA. For a
72 better understanding of the mechanism of photobiological activity, in this study, we used several
73 spectrophotometric techniques, like UV-Vis spectroscopy, fluorescence spectroscopy and FRET
74 (Supporting Information), to determine how the squaraines bind to DNA.

75



76

77

78 **Fig. 1.** Molecular structure of the two investigated squaraines.

79

80 **2. Materials and methods**

81

82 **2.1. Materials**

83

84 Ethidium bromide (EB), calf thymus DNA (ctDNA) and dimethyl sulfoxide (DMSO) were
 85 purchased from Merck and used without further purification. An in-house Millipore system was
 86 used to obtain Millipore grade water (resistivity: 18.2 MΩ cm at 25 °C). Squaraines were
 87 synthesized as previously reported [6]. TNE buffer was obtained using-Picofluor™ protocol. TNE
 88 buffer was prepared by dissolving 12.1 g of Tris, 3.7 g of EDTA and 116.9 g of NaCl in 1 L of
 89 water. The pH of TNE was adjusted to 7.4 with HCl. All dilutions useful to the various analyses in
 90 this study were performed using this particular buffer that provides solutions to the correct ionic
 91 strength.

92

93 **2.2. Sample preparation**

94

95 ctDNA stock solution was obtained by dissolving it in water under stirring and stored at 0-4 °C in
 96 the dark. The concentration of ctDNA stock solution was calculated by measuring the absorbance
 97 at 260 nm and using a molar absorption coefficient of 6600 L mol⁻¹ cm⁻¹. The purity of DNA
 98 solution was checked by calculating the absorbance ratio A_{260}/A_{280} . As the value of the ratio was
 99 between 1.8 and 1.9, thus meaning that ctDNA was satisfactorily free from protein, no further
 100 purification was required [19,20]. All the working solutions were further prepared by diluting the
 101 stock solution in buffer.

102 Squaraines stock solutions (1 mM) were obtained by dissolving the solid in DMSO and dilutions
 103 for the experiments were made in TNE buffer.

104

105 **2.3. Methods**

106

107 **2.3.1. UV-Vis measurements**

108 A UH5300 Hitachi spectrophotometer and a 1 x 1 cm quartz cuvettes were used to record all the
109 absorption measurements. The UV-Vis spectra of squaraines complexed with ctDNA were
110 measured in the 200–700 nm range. Experiments were carried out by keeping a fixed amount of
111 squaraines, 10 μM , in a total volume of 3 mL and subsequently titrated with increasing
112 concentration (0–77.4 μM) of ctDNA.

113

114 **2.3.2. Fluorescence measurements**

115 A Horiba Jobin Yvon Fluorolog 3 spectrofluorophotometer and a 1.0 cm quartz cells were used
116 to record all the fluorescence spectra. The fluorescence of ctDNA-EB complex was obtained in
117 the range 585-750 nm upon excitation at 286 nm; slits were set on 5 nm and 3 nm for excitation
118 and emission, respectively. ctDNA and EB concentrations to form the complex were set at 36.7
119 μM and 10 μM , respectively, in a volume of 3 mL; squaraines concentration was varied from 0–
120 40 μM .

121

122 **2.3.3. Competitive displacement assays**

123 Hoechst 33258 (HOE) was added to a ctDNA solution in order to study the competitive
124 displacement. The HOE-ctDNA complex containing 1 μM HOE and 10 μM ctDNA was excited at
125 355 nm. Emission spectra were recorded in the spectral range 375-600 nm. Squaraine was
126 gradually added (0-200 μM) to a constant concentration of HOE-ctDNA complex. The cuvette was
127 filled with TNE buffer to a final volume of 3 mL.

128

129 **2.3.4. Iodide quenching studies**

130 The iodide quenching tests were accomplished after exciting squaraines and recording the
131 emission spectra in presence of gradually increased amounts of KI, both in absence and presence
132 of ctDNA (50 μM). A total of 3 mL solution comprised 50 μM squaraine, TNE buffer and variable
133 concentration of KI in the range of 0-4 mM. Fluorescence spectra were measured over the
134 spectral range 280-500 nm upon excitation at 260 nm. Fluorescence quenching efficiency both in
135 absence and presence of ctDNA was analyzed using the Stern-Volmer equation.

136

137 **2.3.5. Role of ionic strength**

138 The effect of ionic strength was investigated by changing the concentration of sodium chloride
139 (NaCl) in the range of 0-90 mM, in a total volume of 3 mL containing 50 μM squaraine, 50 μM
140 ctDNA and TNE buffer. Fluorescence spectra were recorded in the spectral range 280-500 nm
141 and the excitation wavelength was set at 260 nm.

142

143 **3. Results and discussion**

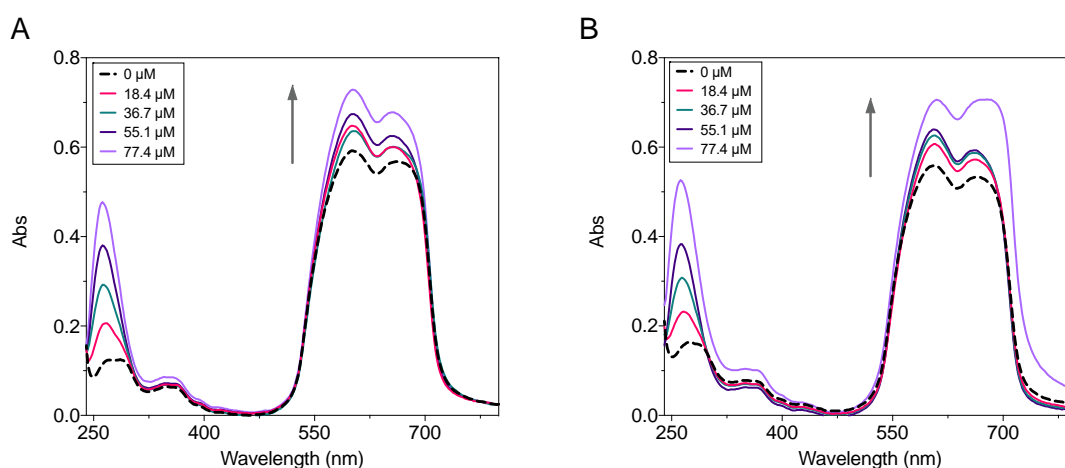
144

145 **3.1. UV-Vis absorption studies**

146

147 UV-Vis spectroscopy is one of the simplest and easily reproducible technique used to assess the
148 type of interaction between macromolecules (usually proteins) and small molecules [21]. Through
149 UV-Vis study the structure and the conformation of complexes can be explored. The absorption
150 spectra of squaraines with and without ctDNA were registered and are displayed in Figure 2.
151 Generally, the bound of small molecules to DNA via intercalation, involves the aromatic groups
152 of the chromophore and the DNA base pairs, of whom mechanism of interaction is stacking-
153 based. The resulting maximum of absorption will display bathochromism and a significant
154 hypochromic effect. When intercalation takes place, the probability of electron transition and
155 coupling energy are reduced, thus resulting in a color reduction and a red-shift phenomenon
156 [2,22,23]. On the other hand, if electrostatic interaction occurs, mainly a hyperchromic effect will
157 be observed as a consequence of the changes of the structure and conformation of DNA upon
158 the formation of the complex between the compound and DNA. Generally speaking, when a
159 positively charged compound bind to the negatively charged phosphate groups of DNA backbone,
160 the secondary structure of DNA will shrink and spectroscopically a hyperchromic effect is usually
161 observed [24,25]. Similarly, the groove binding interaction produces an enhancement of the
162 absorption bands, which is proportional to the concentration of DNA[23]. As shown in Figure 2,
163 with the addition of increasing concentration of ctDNA to a SQ dye solution, no bathochromic
164 shifts or hypochromic effects were observed. Actually, upon increasing the concentration of DNA,
165 we recorded an increase of the absorption bands at 596 and 660 nm corresponding to squaraines.
166 These observations suggest that rather than an intercalative mode of interaction between
167 squaraines and ctDNA, an electrostatic or groove binding mode is preferred.

168



169

170

171 **Figure 2.** UV-Vis spectra of squaraines-ctDNA interaction. In the spectrum (A) it is represented
172 the interaction between ctDNA and Br-C4 and in the spectrum (B) the interaction between ctDNA
173 and I-C4. The black dashed line represents the absorption spectrum of squaraine alone, while
174 the colored lines represent squaraine absorption spectrum at increasing concentrations of ctDNA.
175

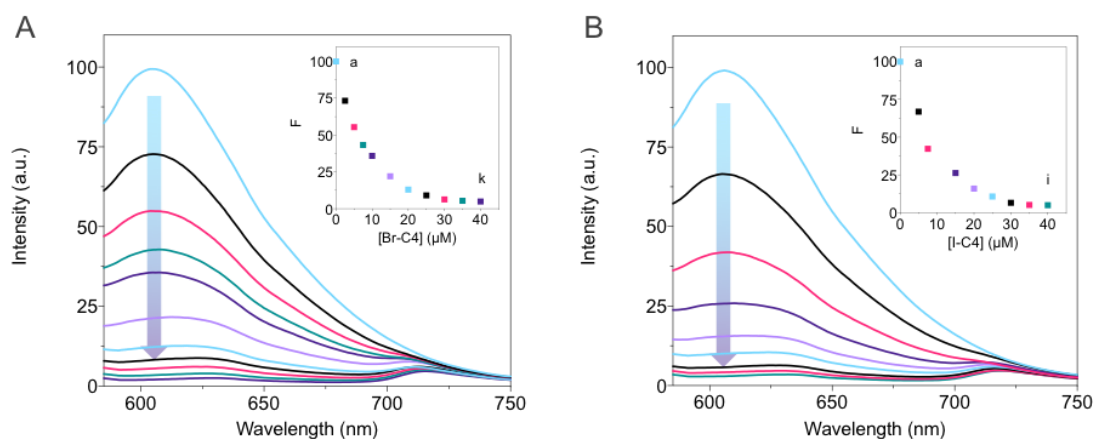
175

176 **3.2. Fluorescence quenching mechanism of SQ-ctDNA-EB system**

177

178 Ethidium bromide (EB) is a planar molecule characterized by a very weak fluorescence in
179 aqueous medium. However, when it intercalates into the base pairs of DNA, it encounters a more
180 hydrophobic environment that forces the loss of any water molecule associated with EB. As water
181 is a very efficient fluorescence quencher the result is a great increase of fluorescence emission
182 [19,26–28]. With this in mind, a complex ctDNA-Ethidium Bromide (EB) was used because the
183 emission spectrum of the ctDNA alone is too low in terms of intensity. The enhanced fluorescence
184 intensity can be turned off by adding a second molecule and the amount of fluorescence
185 quenching can be used to define the binding between the second compound and ctDNA[29].
186 Figure 3 shows the fluorescence spectra of ctDNA-EB complex upon the increasing
187 concentrations of squaraines (SQ). The fluorescence of ctDNA-EB systems at 605 nm decreased
188 as the amount of squaraines increased. The fluorescence quenching data of the complex SQ-
189 ctDNA-EB were analyzed by three different approaches in order to calculate the equilibrium
190 association (K_A) and dissociation (K_D) constants. For the SQ-ctDNA-EB system, two possible
191 reasons describe the reduction of the ctDNA-EB emission upon addition of SQ. The first reason
192 consists in replacement of the intercalated EB from the double strand which decreases the
193 concentration of EB binding to ctDNA. The second reason is the turn off the fluorescence of
194 ctDNA-EB complex by bond of SQ [1]. The absorption measurements suggest that the binding
195 mechanism between SQ and ctDNA was not relying on intercalation but more likely on
196 electrostatic or groove binding modes. Moreover, based on the values of binding constant
197 reported in Table 1, we can state that the replacement of EB from ctDNA was not possible as the
198 binding constant of EB-DNA is $5.16 \times 10^5 \text{ mol L}^{-1}$ as reported by Ramana et al. [19,26], while for
199 the SQ-ctDNA-EB system, binding constant are on average 5 fold lower. To confirm this
200 hypothesis further investigation were conducted.

201



202
203

204 **Figure 3.** Fluorescence spectra of SQ-ctDNA-EB. (A) Interaction between ctDNA-EB and Br-C4
205 and (B) interaction of ct-DNA-EB and I-C4. The most intensive light blue lines represent emission
206 spectra of ctDNA-EB complex; all the other colored lines are the emission spectra of interactions
207 between ctDNA-EB and squaraines. [Br-C4]_{a-k} = 0, 2.5, 5, 7.5, 10, 15, 20, 25, 30, 35, 40 μM; [I-
208 C4]_{a-i} = 0, 5, 7.5, 15, 20, 25, 30, 35, 40 μM. The insets represent the variation of the maximum of
209 fluorescence upon increasing the concentration of squaraine.

210

211 3.2.1. Stern-Volmer equation

212 The fluorescence quenching data of SQ-ctDNA-EB complex were analyzed according to Stern-
213 Volmer equation (Eq.1)

$$214 \quad \frac{F_0}{F} = 1 + K_{SV}[Q] \quad (\text{Eq. 1})$$

215 where F_0 is the fluorescence intensity of ctDNA-EB alone and F is the fluorescence intensity of
216 the complex in presence of increased concentration of squaraine, K_{SV} is the Stern-Volmer
217 quenching constant and $[Q]$ is the squaraine concentration. Quenching data are presented as
218 plots of F_0/F versus $[Q]$, yielding an intercept of one on the y-axis and a slope equal to K_{SV} . The
219 fluorescence quenching of ctDNA-EB upon binding to SQ shows positive deviation from the Stern-
220 Volmer equation. This tendency is often observed when the extent of quenching is large. In such
221 events, usually only the linear part of the plot is fitted to Stern-Volmer equation (insets on Figure
222 4A and 4B), in order to gain information about the SQ-ctDNA-EB interaction constant [30].

223

224 3.2.2. Non-linear least squares

225 Data were fitted also according to a non-linear fit method, based on Equation 2:

$$226 \quad y = \frac{B_{max} \cdot [Q]}{K_D + [Q]} \quad (\text{Eq. 2})$$

227 where, y is the explicit binding obtained by measuring fluorescence intensity, B_{max} is the
228 maximum extent of the complex SQ-ctDNA-EB created at saturation and K_D is the equilibrium

229 dissociation constant. Since in a biomolecular reaction at equilibrium the K_D and K_A are mutually
 230 correlated, we calculated K_A as the reciprocal of K_D . The binding curves are displayed in Figure 4
 231 (C and D); the percentage of bound ctDNA, that is, the ordinate axis, calculated from the emission
 232 maximum intensities, is plotted against the squaraines concentration. The K_A and K_D values are
 233 reported in Table 1.

234

235 3.2.3. Lineweaver-Burk

236 Another frequently used method to linearize data is the Lineweaver–Burk equation based on
 237 Equation 3:

$$238 \frac{1}{(F_0 - F)} = \frac{1}{F_0} + \frac{K_D}{F_0 \cdot [Q]} \quad (Eq. 3)$$

239 In Figure 4 the reciprocals of $F_0 - F$ are plotted against reciprocals of $[Q]$. K_D/F_0 ratio is the slope
 240 of the line while F_0 is the reverse of the intercept. The equilibrium dissociation (K_D) and association
 241 (K_A) constants are thus easily calculated and are reported in Table 1.

242 As reported in Table 1, we can observe that constants obtained with different analysis methods
 243 perfectly agree to each other. Association constants are in the order of 10^5 M^{-1} which is
 244 appreciably lower than that of the intercalation binding mode. The K_A of classic intercalators such
 245 as ruthenium complexes are reported to be around 10^6 M^{-1} [31,32], while even higher values on
 246 the order of 10^7 M^{-1} were reported for anthracycline as daunorubicin [33,34]. The value of the
 247 obtained binding constants is an indirect confirmation of the mode of interaction of squaraine with
 248 DNA.

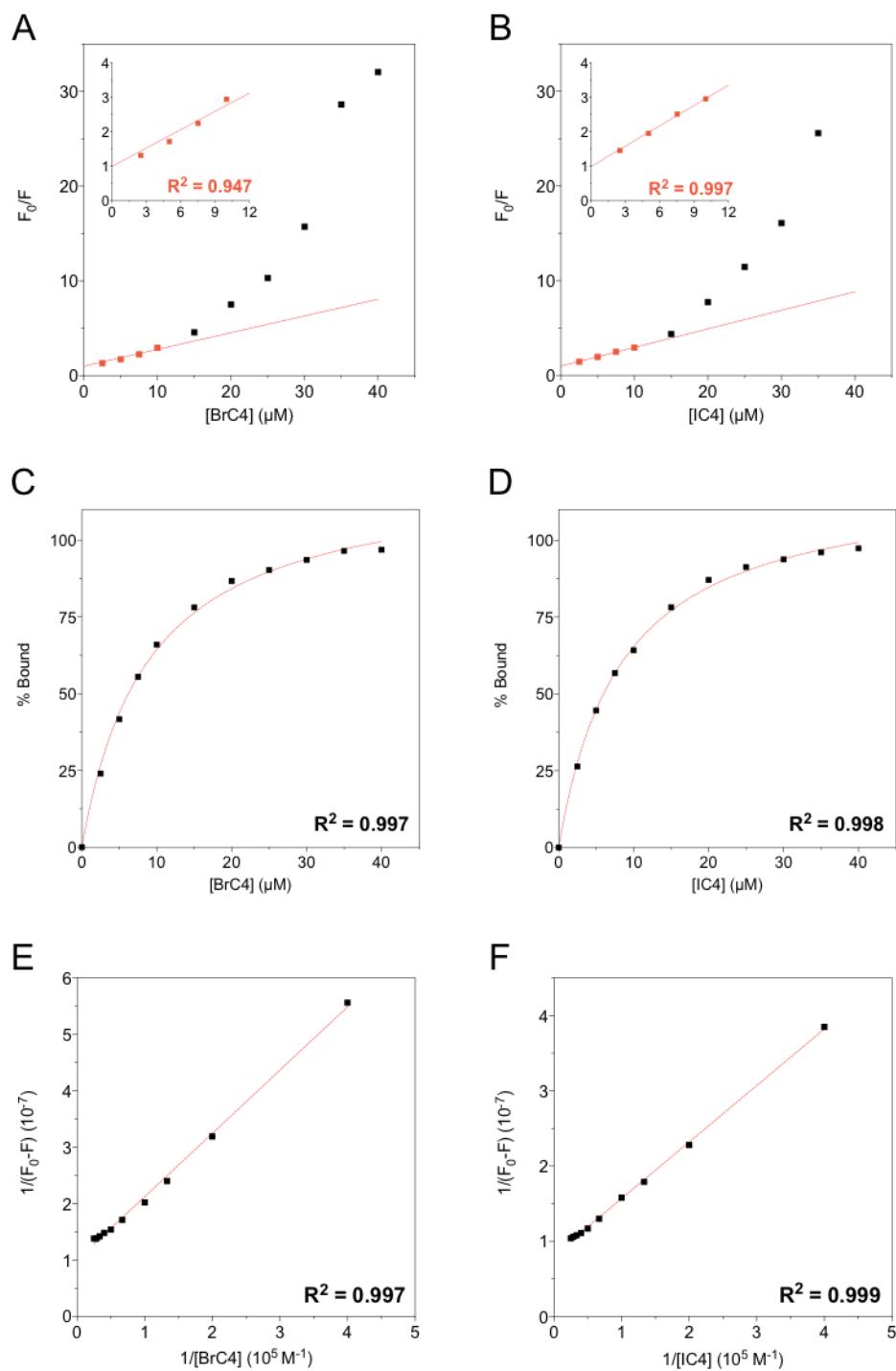
249

250 **Table 1.** Association (K_A) and Dissociation (K_D) constants at 25 °C calculated with different
 251 mathematical models.

252

	Stern-Volmer	Non-Linear Fit		Lineweaver-Burk	
	K_{SV}	K_D	K_A	K_D	K_A
	($\cdot 10^5 \text{ M}^{-1}$)	($\cdot 10^{-6} \text{ M}$)	($\cdot 10^5 \text{ M}^{-1}$)	($\cdot 10^{-6} \text{ M}$)	($\cdot 10^5 \text{ M}^{-1}$)
Br-C4	2.10	8.40	1.19	8.92	1.12
I-C4	2.09	7.39	1.35	8.38	1.19

253



254
255

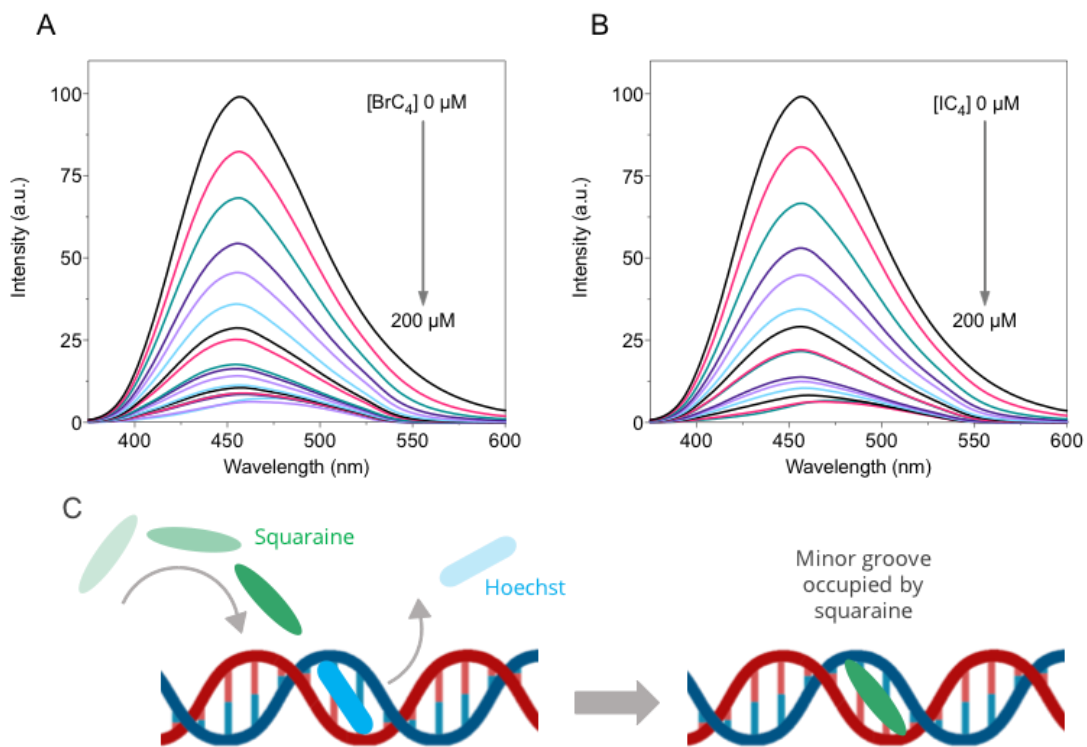
256 **Figure 4.** Data analysis of fluorescence quenching. In the spectra (A) and (B) are represented
 257 the Stern-Volmer analysis of BrC4-ctDNA-Eb and IC4-ctDNA-Eb interactions, respectively. The
 258 insets on (A) and (B) reports the linear tract of the Stern-Volmer plot. In the spectra (C) and (D)
 259 are represented the non-linear least squares analysis of the same interactions. At last, in the
 260 spectra (E) and (F) are represented the Lineweaver-Burk analysis of the interactions.

261 **3.3 Competitive Displacement Assay**

262

263 To better understand how squaraines bind DNA, we carried out competitive binding experiments.
264 In this experiment, Hoechst 33258, a commonly used minor groove binder of DNA with high
265 specificity for AT-rich sequences, was employed to study the competitive replacement by groove
266 binders [1,20,21]. Hoechst 33258 has a very weak fluorescence intensity in aqueous solutions
267 however, on binding with DNA, it shows an increase in the fluorescence intensity characterized
268 by a strong band at 458 nm [26,35]. Molecules that bind DNA via groove binding mode can replace
269 Hoechst 33258 from the minor groove of DNA that resulting in quenching of fluorescence of the
270 band at 458 nm, which corresponds to the DNA-Hoechst system. As shown in Figure 5, upon
271 addition of gradually increased squaraine concentration, the fluorescence intensity of Hoechst-
272 ctDNA complex was found to diminish. This spectroscopic response can be explained as
273 squaraines gradually replaced the groove bounded dye from ctDNA. This result suggests that
274 rather than intercalation, there is a high probability that the binding of squaraine to ctDNA involves
275 the minor groove sites, as indeed proved by squaraine ability to displace Hoechst. This hypothesis
276 was further evaluated by performing iodide quenching experiment.

277



278

279

280 **Figure 5.** Fluorescent intensity of Hoechst-ctDNA in presence of increasing concentrations of Br-
281 C4 (A) and I-C4 (B). [Br-C4]_{a-r} = 0, 5, 10, 15, 20, 25, 30, 35, 40, 45, 50, 60, 70, 80, 90, 100, 150,

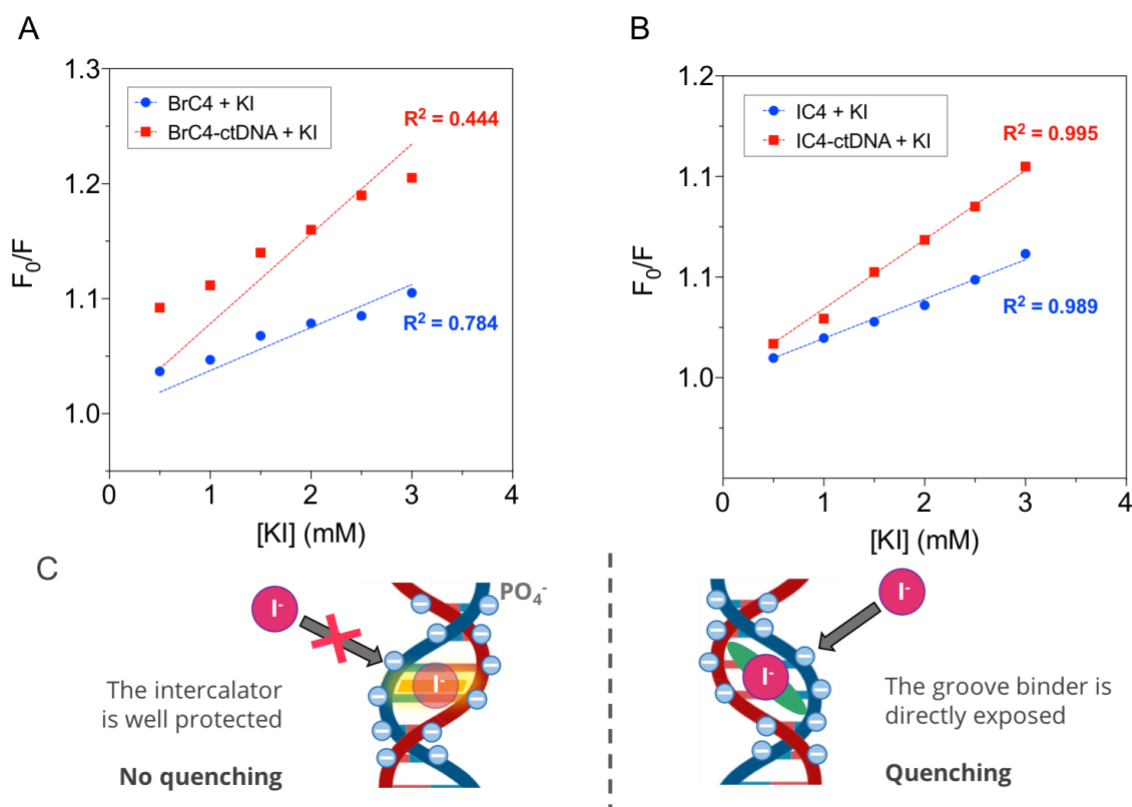
282 200 μM ; $[\text{I-C4}]_{\text{a-o}} = 0, 5, 10, 15, 20, 25, 30, 35, 40, 50, 60, 80, 100, 150, 200 \mu\text{M}$. Schematic
283 representation of the displacement of Hoechst by squaraine on the minor groove (C).

284

285 **3.4 Iodide Quenching Study**

286

287 Iodide ion quenching experiments are useful on understanding if the location of the bonded
288 molecules is placed either outside or inside of DNA helix. Iodide ions are known to turn off the
289 fluorescence of small compounds in aqueous environments. When DNA is present, the negative
290 charges on the phosphate groups repel the iodide ions. If a small compound intercalates the
291 double strand of DNA, then it will be well protected, as the contact with negatively charged
292 molecules (such as iodide ions) toward such compound will be restricted because of electrostatic
293 repulsion. Though, molecules that bind DNA preferably by groove binding or electrostatic
294 mechanism, meaning that these molecules are exposed to the surrounding environment, will be
295 susceptible to the attack of quenchers present in the free medium even when DNA is present
296 [20,21]. The level of accessibility of small compounds to negatively charged quenchers in the
297 environment and in presence of ctDNA is described by K_{SV} that can be calculated using Stern-
298 Volmer equation (see Eq. 1 and Figure 6). Reduction in the magnitude of K_{sv} in presence of DNA
299 is achieved with intercalation, though for groove binders or electrostatic interaction, it remains
300 mostly unaffected. In Figure 6, is reported that KI could efficiently quench the emission of
301 squaraines. However, the presence of ctDNA, produce a slight increase of the K_{sv} value. The
302 calculated K_{sv} values in the absence and presence of ctDNA for Br-C4 by KI was found to be 38
303 and 70 M respectively, while for I-C4 the K_{sv} values are 20 and 34 mol L^{-1} respectively. The
304 magnitude of quenching of squaraines that we observe in the presence and in the absence of
305 ctDNA is almost unchanged and therefore, there is a higher probability that the interaction of
306 squaraines with DNA take place outside the DNA helix. Taking together the competitive
307 displacement assay and the iodide quenching study, we can state with more confidence that the
308 binding of squaraines to ctDNA is mainly guided by groove binding interaction.



309
310

311 **Figure 6.** Stern-Volmer plots for fluorescence quenching of Br-C4 (A) and I-C4 (B) by KI in the
312 absence and presence of ctDNA (50 μ M). Concentrations of KI was varied from 0.5 to 3 mM.
313 Schematic representation of the mechanism of quenching of fluorescence of the groove binders
314 by action of iodide (C). While intercalators are well protected by being inserted between
315 nucleotides, groove binders are directly exposed to the surrounding environment.

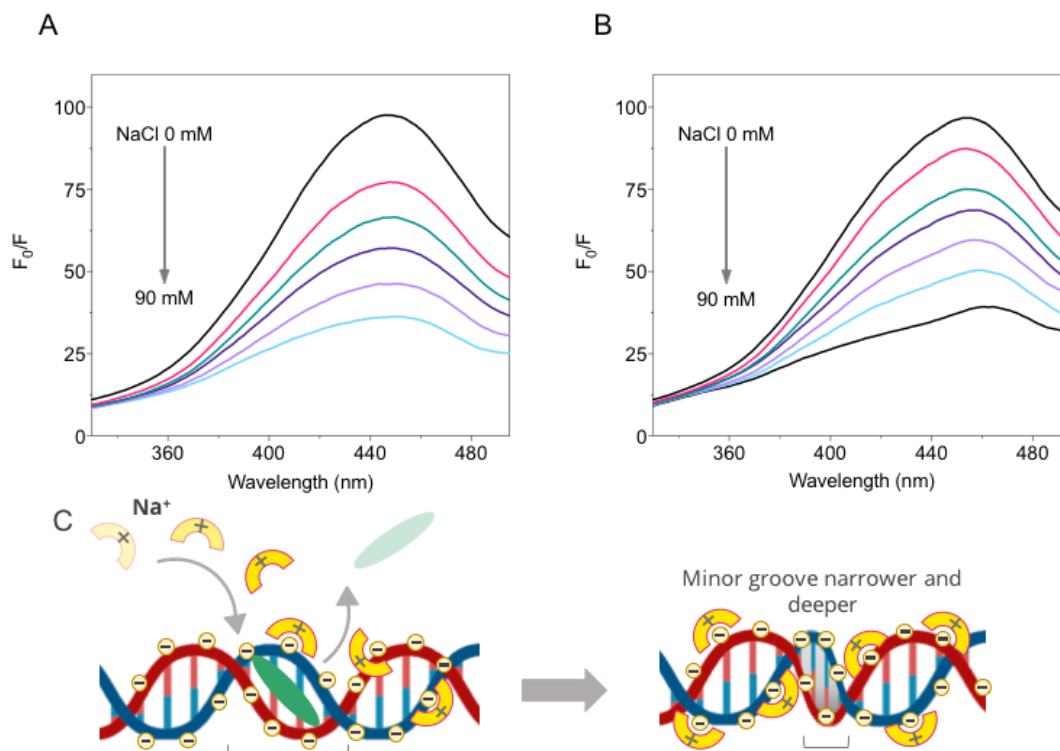
316

317 3.5 Effect of Ionic Strength

318

319 Another methodology used to discriminate the binding between small compounds and ctDNA is
320 the investigation of ionic strength on the system. Normally, strong electrolyte as sodium chloride
321 (NaCl) is used for this assay. After solubilization, Na⁺ partially neutralizes the anionic helix of DNA
322 so reducing the electrostatic repulsion between DNA strands. Small molecules that intercalate
323 into the adjacent base pairs of DNA will be shielded from the surrounding solvent and so the
324 emission intensity will be almost unvaried with the increasing of the concentration of NaCl [36]. In
325 case of surface binding molecules, particularly for electrostatic-dependent binding, the bound with
326 DNA takes place outside the groove; in this case NaCl will reduce the interaction which will be
327 translated in the reduction of emission intensity. Nonetheless, for groove binding molecules, with
328 the increasing of the concentration of NaCl a proportional decrease of fluorescence intensity is
329 usually observed. The increased ionic strength shrinks and deepens the DNA grooves. The

330 induced structure modification of the helix cause the release of the groove bonded molecule and
 331 that translates in the decrease of fluorescence intensity [11,37]. So, the effect of NaCl on the
 332 fluorescence of ctDNA-squaraine were studied. The experimental results indicate that the
 333 fluorescence intensities of ctDNA-squaraine was decreased with increasing of NaCl concentration
 334 (Figure 7). These results can further confirm that the interaction between ctDNA and squaraines
 335 is groove binding related.
 336



337
 338
 339 **Figure 7.** Effects of ionic strength on the fluorescence intensity of Br-C4-ctDNA (A) and I-C4-
 340 ctDNA (B). Schematic representation of the ionic strength on the structure of DNA and the
 341 implication of squaraine accommodation into the minor groove (C).

342

343 4. Conclusions

344

345 In this study the interaction between ctDNA and Br- and I-C4 squaraines has been studied through
 346 different spectroscopic techniques. Based on the data collected by absorption and emission
 347 spectroscopies, displacement assay, iodide quenching study, ionic strength effect and FRET
 348 (Supporting Information) data, we can state that the binding mode of squaraine with DNA was
 349 disclosed as minor groove binding. The squaraines have a K_A order of 10^5 M^{-1} . Considering that
 350 the order of magnitude of association constant of groove binders is usually known to be around
 351 10^3 M^{-1} [38,39], we conclude that Br- and I-C4 have quite a high affinity for ctDNA. This work is

352 expected to provide deeper insight into understanding the mechanism of interaction of squaraines
353 with DNA and the knowledge gained from this study could be used for the development of
354 potential probes for DNA as well as more selective and efficient photodynamic therapy agents.

355

356 **Declaration of competing interests**

357

358 The authors declare that they have no known competing financial interests or personal
359 relationships that could have appeared to influence the work reported in this paper.

360

361 **Acknowledgments**

362

363 The authors acknowledge the financial support from the University of Torino (Ricerca Locale ex-
364 60%, Bando 2019) and from the Fondazione Cassa di Risparmio (CRT) di Torino, Italy.

365

366

367

368 **References**

369

370

371 [1] M.M.V. Ramana, R. Betkar, A. Nimkar, P. Ranade, B. Mundhe, S. Pardeshi, In vitro DNA
372 binding studies of antiretroviral drug nelfinavir using ethidium bromide as fluorescence
373 probe, *J. Photochem. Photobiol. B Biol.* 151 (2015) 194–200.

374 <https://doi.org/10.1016/j.jphotobiol.2015.08.012>.

375 [2] K. Nakamoto, M. Tsuboi, G.D. Strahan, *Drug–DNA Interactions: Structures and Spectra*,
376 Wiley, 2008.

377 [3] A.M. Rkein, D.M. Ozog, *Photodynamic Therapy, Dermatol. Clin.* 32 (2014) 415–425.

378 <https://doi.org/10.1016/j.det.2014.03.009>.

379 [4] H. Abrahamse, M.R. Hamblin, *New photosensitizers for photodynamic therapy*,

380 *Biochem. J.* 473 (2016) 347–364. <https://doi.org/10.1042/BJ20150942>.

381 [5] R.R. Avirah, D.T. Jayaram, N. Adarsh, D. Ramaiah, *Squaraine dyes in PDT: from basic
382 design to in vivo demonstration*, *Org. Biomol. Chem.* 10 (2012) 911–920.

383 <https://doi.org/10.1039/C1OB06588B>.

384 [6] L. Serpe, S. Ellena, N. Barbero, F. Foglietta, F. Prandini, M.P. Gallo, R. Levi, C. Barolo,

385 R. Canaparo, S. Visentin, *Squaraines bearing halogenated moieties as anticancer*

386 *photosensitizers: Synthesis, characterization and biological evaluation*, *Eur. J. Med.*

387 *Chem.* 113 (2016) 187–197. <https://doi.org/10.1016/j.ejmech.2016.02.035>.

388 [7] B. Ciubini, S. Visentin, L. Serpe, R. Canaparo, A. Fin, N. Barbero, *Design and synthesis
389 of symmetrical pentamethine cyanine dyes as NIR photosensitizers for PDT*, *Dye*.

- Pigment. 160 (2019) 806–813. <https://doi.org/10.1016/j.dyepig.2018.09.009>.
- [8] J. Park, N. Barbero, J. Yoon, E. Dell’Orto, S. Galliano, R. Borrelli, J.H. Yum, D. Di Censo, M. Grätzel, M.K. Nazeeruddin, C. Barolo, G. Viscardi, Panchromatic symmetrical squaraines: A step forward in the molecular engineering of low cost blue-greenish sensitizers for dye-sensitized solar cells, *Phys. Chem. Chem. Phys.* 16 (2014) 24173–24177. <https://doi.org/10.1039/c4cp04345f>.
- [9] J. Park, C. Barolo, F. Sauvage, N. Barbero, C. Benzi, P. Quagliotto, S. Coluccia, D. Di Censo, M. Grätzel, M.K. Nazeeruddin, G. Viscardi, Symmetric vs. asymmetric squaraines as photosensitisers in mesoscopic injection solar cells: A structure-property relationship study, *Chem. Commun.* 48 (2012) 2782–2784. <https://doi.org/10.1039/c2cc17187b>.
- [10] D. Saccone, S. Galliano, N. Barbero, P. Quagliotto, G. Viscardi, C. Barolo, Polymethine Dyes in Hybrid Photovoltaics: Structure–Properties Relationships, *European J. Org. Chem.* 2016 (2016) 2244–2259. <https://doi.org/10.1002/ejoc.201501598>.
- [11] S. Kashanian, S. Javanmardi, A. Chitsazan, M. Paknejad, K. Omidfar, Fluorometric study of fluoxetine DNA binding, *J. Photochem. Photobiol. B Biol.* 113 (2012) 1–6. <https://doi.org/10.1016/j.jphotobiol.2012.04.002>.
- [12] N. Barbero, C. Butnarusu, S. Visentin, C. Barolo, Squaraine Dyes: Interaction with Bovine Serum Albumin to Investigate Supramolecular Adducts with Aggregation-Induced Emission (AIE) Properties, *Chem. - An Asian J.* 14 (2019) 896–903. <https://doi.org/10.1002/asia.201900055>.
- [13] M. Shimi, V. Sankar, M.K.A. Rahim, P.R. Nitha, S. Das, K. V. Radhakrishnan, K.G. Raghu, Novel glycoconjugated squaraine dyes for selective optical imaging of cancer cells, *Chem. Commun.* 53 (2017) 5433–5436. <https://doi.org/10.1039/c6cc10282d>.
- [14] G.M. Paternò, L. Moretti, A.J. Barker, C. D’Andrea, A. Luzio, N. Barbero, S. Galliano, C. Barolo, G. Lanzani, F. Scotognella, Correction: Near-infrared emitting single squaraine dye aggregates with large Stokes shifts, *J. Mater. Chem. C* 5 (2017) 11144. <https://doi.org/10.1039/C7TC90165H>.
- [15] G. Alberto, N. Barbero, C. Divieto, E. Rebba, M.P. Sassi, G. Viscardi, G. Martra, Solid silica nanoparticles as carriers of fluorescent squaraine dyes in aqueous media: Toward a molecular engineering approach, *Colloids Surfaces A Physicochem. Eng. Asp.* 568 (2019) 123–130. <https://doi.org/10.1016/j.colsurfa.2019.01.052>.
- [16] D. Ramaiah, I. Eckert, K.T. Arun, L. Weidenfeller, B. Epe, Squaraine Dyes for Photodynamic Therapy: Study of Their Cytotoxicity and Genotoxicity in Bacteria and Mammalian Cells, *Photochem. Photobiol.* 76 (2002) 672–677. [https://doi.org/10.1562/0031-8655\(2002\)0760672SDFPTS2.0.CO2](https://doi.org/10.1562/0031-8655(2002)0760672SDFPTS2.0.CO2).
- [17] I. Miletto, A. Fraccarollo, N. Barbero, C. Barolo, M. Cossi, L. Marchese, E. Gianotti, Mesoporous silica nanoparticles incorporating squaraine-based photosensitizers: a

- 428 combined experimental and computational approach, *Dalt. Trans.* 47 (2018) 3038–3046.
429 <https://doi.org/10.1039/C7DT03735J>.
- 430 [18] D. Ramaiah, I. Eckert, K.T. Arun, L. Weidenfeller, B. Epe, Squaraine Dyes for
431 Photodynamic Therapy: Mechanism of Cytotoxicity and DNA Damage Induced by
432 Halogenated Squaraine Dyes Plus Light (>600 nm), *Photochem. Photobiol.* 79 (2004)
433 99. [https://doi.org/10.1562/0031-8655\(2004\)79<99:sdfptm>2.0.co;2](https://doi.org/10.1562/0031-8655(2004)79<99:sdfptm>2.0.co;2).
- 434 [19] Y. Cui, E. Hao, G. Hui, W. Guo, F. Cui, Investigations on the interactions of diclofenac
435 sodium with HSA and ctDNA using molecular modeling and multispectroscopic methods,
436 *Spectrochim. Acta Part A Mol. Biomol. Spectrosc.* 110 (2013) 92–99.
437 <https://doi.org/10.1016/J.SAA.2013.01.093>.
- 438 [20] S.U. Rehman, T. Sarwar, H.M. Ishqi, M.A. Husain, Z. Hasan, M. Tabish, Deciphering the
439 interactions between chlorambucil and calf thymus DNA: A multi-spectroscopic and
440 molecular docking study, *Arch. Biochem. Biophys.* 566 (2015) 7–14.
441 <https://doi.org/10.1016/j.abb.2014.12.013>.
- 442 [21] M.A. Husain, T. Sarwar, S.U. Rehman, H.M. Ishqi, M. Tabish, Ibuprofen causes
443 photocleavage through ROS generation and intercalates with DNA: a combined
444 biophysical and molecular docking approach, *Phys. Chem. Chem. Phys.* 17 (2015)
445 13837–50. <https://doi.org/10.1039/c5cp00272a>.
- 446 [22] R. Arif, P.S. Nayab, Akrema, M. Abid, U. Yadava, Rahisuddin, Investigation of DNA
447 binding and molecular docking propensity of phthalimide derivatives: in vitro antibacterial
448 and antioxidant assay, *J. Anal. Sci. Technol.* 10 (2019) 1–9.
449 <https://doi.org/10.1186/s40543-019-0177-1>.
- 450 [23] Y. Yang, J.Y. Bian, Y.H. Li, H.C. Guan, Y.R. Tang, Y.L. Chen, S.M. Yue, Construction of
451 six complexes from 2-(2-pyridyl)benzothiazole and polycarboxylic acids: Synthesis,
452 crystal structures and DNA-binding properties, *J. Mol. Struct.* (2020).
453 <https://doi.org/10.1016/j.molstruc.2019.127219>.
- 454 [24] F. Arjmand, A. Jamsheera, DNA binding studies of new valine derived chiral complexes
455 of tin(IV) and zirconium(IV), *Spectrochim. Acta - Part A Mol. Biomol. Spectrosc.* (2011).
456 <https://doi.org/10.1016/j.saa.2010.06.009>.
- 457 [25] M. Sirajuddin, S. Ali, A. Badshah, Drug–DNA interactions and their study by UV–Visible,
458 fluorescence spectroscopies and cyclic voltametry, *J. Photochem. Photobiol. B Biol.* 124
459 (2013) 1–19. <https://doi.org/10.1016/J.JPHOTOBIOLOG.2013.03.013>.
- 460 [26] M.M.V. Ramana, R. Betkar, A. Nimkar, P. Ranade, B. Mundhe, S. Pardeshi, Synthesis of
461 a novel 4H-pyran analog as minor groove binder to DNA using ethidium bromide as
462 fluorescence probe, *Spectrochim. Acta - Part A Mol. Biomol. Spectrosc.* 152 (2016) 165–
463 171. <https://doi.org/10.1016/j.saa.2015.07.037>.
- 464 [27] R. Gaur, M. Usman, A combined experimental and theoretical investigation of
465 ruthenium(II)-hydrazone complex with DNA: Spectroscopic, nuclease activity,

- 466 topoisomerase inhibition and molecular docking, *Spectrochim. Acta Part A Mol. Biomol.*
467 *Spectrosc.* 209 (2019) 100–108. <https://doi.org/10.1016/J.SAA.2018.10.035>.
- 468 [28] J. Olmsted, D.R. Kearns, Mechanism of Ethidium Bromide Fluorescence Enhancement
469 on Binding to Nucleic Acids, *Biochemistry.* 16 (1977) 3647–3654.
- 470 [29] M.M. Aleksić, V. Kapetanović, An overview of the optical and electrochemical methods
471 for detection of DNA - Drug interactions, *Acta Chim. Slov.* 61 (2014) 555–573.
- 472 [30] M. Airoidi, G. Barone, G. Gennaro, A.M. Giuliani, M. Giustini, Interaction of doxorubicin
473 with polynucleotides. a spectroscopic study, *Biochemistry.* 53 (2014) 2197–2207.
474 <https://doi.org/10.1021/bi401687v>.
- 475 [31] S. Mardanya, S. Karmakar, D. Maity, S. Baitalik, Ruthenium(II) and osmium(II) mixed
476 chelates based on pyrenyl-pyridylimidazole and 2,2'-bipyridine ligands as efficient DNA
477 intercalators and anion sensors, *Inorg. Chem.* 54 (2015) 513–526.
478 <https://doi.org/10.1021/ic502271k>.
- 479 [32] E. Wachter, D. Moyá, S. Parkin, E.C. Glazer, Ruthenium Complex “Light Switches” that
480 are Selective for Different G-Quadruplex Structures, *Chem. - A Eur. J.* 22 (2016) 550–
481 559. <https://doi.org/10.1002/chem.201503203>.
- 482 [33] Y. Lu, J. Lv, G. Zhang, G. Wang, Q. Liu, Interaction of an anthracycline disaccharide with
483 ctDNA: Investigation by spectroscopic technique and modeling studies, *Spectrochim.*
484 *Acta - Part A Mol. Biomol. Spectrosc.* 75 (2010) 1511–1515.
485 <https://doi.org/10.1016/j.saa.2010.02.008>.
- 486 [34] A.A. Almaqwashi, T. Paramanathan, I. Rouzina, M.C. Williams, Mechanisms of small
487 molecule-DNA interactions probed by single-molecule force spectroscopy, *Nucleic Acids*
488 *Res.* 44 (2016) 3971–3988. <https://doi.org/10.1093/nar/gkw237>.
- 489 [35] J.H. Shi, J. Chen, J. Wang, Y.Y. Zhu, Binding interaction between sorafenib and calf
490 thymus DNA: Spectroscopic methodology, viscosity measurement and molecular
491 docking, *Spectrochim. Acta - Part A Mol. Biomol. Spectrosc.* (2015).
492 <https://doi.org/10.1016/j.saa.2014.09.056>.
- 493 [36] N. Akbay, Z. Seferoğlu, E. Gök, Fluorescence interaction and determination of calf
494 thymus DNA with two ethidium derivatives, *J. Fluoresc.* 19 (2009) 1045–1051.
495 <https://doi.org/10.1007/s10895-009-0504-9>.
- 496 [37] S. Bi, T. Zhao, Y. Wang, H. Zhou, B. Pang, T. Gu, Binding studies of terbutaline sulfate
497 to calf thymus DNA using multispectroscopic and molecular docking techniques,
498 *Spectrochim. Acta - Part A Mol. Biomol. Spectrosc.* (2015).
499 <https://doi.org/10.1016/j.saa.2015.06.042>.
- 500 [38] D. Sahoo, P. Bhattacharya, S. Chakravorti, Quest for mode of binding of 2-(4-
501 (dimethylamino)styryl)-1-methylpyridinium iodide with calf thymus DNA, *J. Phys. Chem.*
502 *B.* 114 (2010) 2044–2050. <https://doi.org/10.1021/jp910766q>.
- 503 [39] B. Jana, S. Senapati, D. Ghosh, D. Bose, N. Chattopadhyay, Spectroscopic exploration

504 of mode of binding of ctDNA with 3-hydroxyflavone: A contrast to the mode of binding
505 with flavonoids having additional hydroxyl groups, J. Phys. Chem. B. 116 (2012) 639–
506 645. <https://doi.org/10.1021/jp2094824>.
507